Journal of Anatolian Environmental and Animal Sciences
(*Anadolu Çevre ve Hayvancılık Bilimleri Dergisi*)
https://doi.org/10.35229/jaes.1848473

JAES
Year: 11, 2026 (1-8)
AÇEH
Yıl: 11, 2026 (1-8)

ARAŞTIRMA MAKALESİ RESEARCH PAPER

Rize-Sourced Hazelnut Shell Ash as a Green Corrosion Inhibitor for Fe Metal in 1 % NaCl: Electrochemical Evaluation and Mechanistic Insights

Turan YANARDAĞ[1]* | Bedia Semra TAŞCI[2] | Müşerref ÖNAL[3] | Işıl Deniz ULUSOY[4] Müşerref KİRİŞ[5] | Nilseli ÖZTÜRK[6]

[1,3,5,6]*Ankara University Faculty of Science Department of Chemistry, 06100, Ankara, Türkiye*
[2]*Fatma Yaşar Önen Trade Vocational and Technical Anatolian High School, 06590, Ankara, Türkiye*
[4]*Ankara University Technocity, Bahçelievler District, 06830, Ankara, Türkiye*

Received: *26.12.2025* ***Published:*** *12.03.2026*

How to cite: **Yanardağ, T., Taşcı, B.S., Önal, M., Ulusoy, I.D., Kiriş, M., & Öztürk, N. (2026).** Rize-Sourced Hazelnut Shell Ash as a Green Corrosion Inhibitor for Fe Metal in 1 % NaCl: Electrochemical Evaluation and Mechanistic Insights. *J. Anatolian Envion. Anim. Sci.,* ***11,*** 1-8. https://doi.org/10.35229/jaes.1848473

Atıf yapmak için: **Yanardağ, T., Taşcı, B.S., Önal, M., Ulusoy, I.D., Kiriş, M., & Öztürk, N. (2026).** Fe Metali İçin Yeşil Korozyon İnhibitörü Olarak Rize Kaynaklı Fındık Kabuğu Külünün %1 NaCl Ortamında: Elektrokimyasal Değerlendirilmesi ve Mekaniksel Yaklaşımları. *Anadolu Çev. Hay. Bil. Derg.*, ***11***, 1-8. https://doi.org/10.35229/jaes.1848473

***Corresponding author's:**
Turan YANARDAĞ
Ankara University Faculty of Science
Department of Chemistry, 06100, Ankara, Türkiye
✉: tyanardag@ankara.edu.tr

Abstract: The corrosion behavior of iron (Fe) in 300 mL of 1% NaCl solution containing different concentrations of hazelnut shell ash (HSA) 3.34% (v/v), 8.34% (v/v), and 25% (v/v) was investigated at 25°C using electrochemical techniques. The investigations carried out using open-circuit potential (E_{OCP}), electrochemical impedance spectroscopy (EIS), and current–potential (Tafel) polarization techniques. The results showed that the addition of HSA significantly shifted the potential of the Fe in the cathodic direction and raised the pH of the solution (pH 5.8 to ~10) at all concentrations. Furthermore, containing 3.34 % of HSA, the corrosion rate (i_{corr}) decreased from 0.50 µA cm^{-2} to 0.15 µA cm^{-2} according to Tafel results, Fe corrosion decreased by approximately 70%. Inductively coupled plasma mass spectrometry (ICP-MS) analyses revealed that Fe, Ni, Cr, and Co heavy metal ions migrated into the working solution; it was determined that the addition of HSA significantly reduced the concentration of these ions in the solution. The decrease was particularly pronounced for Fe ions; Fe^{2+}/Fe^{3+} concentrations decreased from 203 ppb to <33 ppb (25% v/v), <35 ppb (8.34% v/v) and <22 ppb (3.34% v/v), respectively. The detection of lower ion concentrations at 3.34 % HSA indicated that HSA has a high inhibitory effect. These results demonstrated that HSA is an effective candidate for 'green inhibitor' in terms of reducing corrosion and can significantly reduce environmental impact by limiting the release of heavy metal into the environment. The ICP-MS findings found to be highly consistent with the electrochemical methods.

Keywords: Corrosion resistance, ecology, hazelnut shell ash, ICP-MS, inhibitor, iron.

Fe Metali İçin Yeşil Korozyon İnhibitörü Olarak Rize Kaynaklı Fındık Kabuğu Külünün %1 NaCl Ortamında: Elektrokimyasal Değerlendirilmesi ve Mekaniksel Yaklaşımları

***Sorumlu yazar:**
Turan YANARDAĞ
Ankara Üniversitesi, Fen Fakültesi, Kimya Bölümü, Fizikokimya Anabilim Dalı, Ankara, Türkiye
✉: tyanardag@ankara.edu.tr

Öz: Farklı konsantrasyonlarda fındık kabuğu külü (HSA) 3,34% (v/v), 8,34% (v/v) ve 25% (v/v) içeren 300 mL %1 NaCl çözeltisinde demirin (Fe) korozyon davranışı, 25°C'de elektrokimyasal teknikler kullanılarak incelenmiştir. Bu teknikler, açık devre potansiyeli (E_{OCP}), Elektrokimyasal Empedans Spektroskopisi (EIS) ve akım–potansiyel (Tafel) polarizasyon ölçümleri ile gerçekleştirildi. Elde edilen sonuçlar, HSA ilavesinin Fe elektrodunun potansiyelini belirgin biçimde katodik yönde kaydırdığını ve tüm konsantrasyonlarda çözeltinin pH'ını yükselterek ortamı bazik hale getirdiğini (pH 5.8 den ~10'a) gösterdi. Ayrıca, 3.34 % HSA içeren çözeltide, Tafel sonuçlarına göre demirin korozyon hızı (i*corr*) 0.50 $\mu A \cdot cm^{-2}$'den 0.15 $\mu A \cdot cm^{-2}$'ye düştü ve demirin korozyonu yaklaşık %70 oranında azaldı. İndüktif eşleşmiş plazma kütle spektrometresi (ICP-MS) analizleri, Fe, Ni, Cr ve Co ağır metal iyonlarının çalışma çözeltisine geçtiğini ortaya koymuş; HSA ilavesinin bu iyonların çözeltideki derişimini önemli ölçüde azalttığı belirlendi. Azalma özellikle Fe iyonları için belirgindir; Fe^{2+}/Fe^{3+} konsantrasyonları 203 ppb'den sırasıyla <33 ppb (25%), <35 ppb (8,34%) and <22 ppb (3,34%), seviyelerine düştü. İyon derişimlerinin 3,34% (v/v) HSA'da daha düşük tespit edilmesi, HSA'nın inhibitör etkinliğinin yüksek olduğunu gösterdi. Bu sonuçlar, HSA'nın korozyonu azaltma açısından etkili bir "yeşil inhibitör" adayı olduğunu ve ağır metalin ortama yayılımını sınırlandırarak çevresel etkiyi önemli ölçüde azaltabileceğini gösterdi. ICP-MS bulgularının elektrokimyasal verilerle yüksek düzeyde tutarlılık gösterdiği belirlendi.

Keywords: Demir, ekoloji, fındık kabuğu külü, ICP-MS, inhibitör, korozyon direnci.

INTRODUCTION

Corrosion is the deterioration of metal and alloy materials as a result of their interaction with environmental conditions (air, water, humidity, salt, acid, microorganisms, etc.). Therefore, corrosion is a field of science and engineering directly related to the environments. In recent years, numerous experimental and theoretical density functional theory (DFT) studies have been conducted to prevent material corrosion by utilizing the green inhibitor properties of shelled fruits (Shahmoradi et al., 2021; Cartagena et al., 2023; Dai et al., 2023; Furtado et al., 2024; Topuz et al., 2025; Chyhyrynets et al., 2025). The main reason for this interest is that the increase in the production of shelled fruits worldwide may pose an environmental threat due to the waste generated. This increase is particularly evident in hazelnut production in Turkey. Hazelnuts are widely grown in Turkey along the Black Sea coast in the provinces of Rize, Artvin, Giresun, Ordu, and Trabzon. Among hard-shelled fruits, hazelnuts (*Corylus avellana L.*), belonging to the *Betulaceae* family, produced 420,000 tons in 2016, 515,000 tons in 2018, and 650,000 tons in 2023 in Türkiye (Şeker et al., 2023). According to the Food and Agriculture Organization of the United Nations (FAO, 2025) Statistical Corporate Database (FAOSTAT), global hazelnut production has demonstrated consistent upward trend. Türkiye leads the world in hazelnut production with a 63.5% share, followed by Italy with 7.86%, the United States with 6.53%, and Azerbaijan with 6.28% (Çukur et al., 2023). Furthermore, the sufficiency rate of hazelnuts is much higher than that of wheat, barley, maize and soybeans (TÜİK, 2024). The high yield in Türkiye is due to geographical suitability as well as the fact that it is cultivated as a multi-stemmed shrub (Açkurt et al., 1999; Alasalvar et al., 2009; Surek & Buyukkileci, 2017). In other countries, it is mostly cultivated as single-stemmed tree. Due to Türkiye's leading position in global hazelnut production, large quantities of hazelnut shells emerge as agricultural waste each year. Efforts to minimize frost damage in the high-altitude regions of the Black Sea (liming, fumigation) and the provision of Agricultural Insurance (TARSİM) encourage production. Research into irrigation and storage for higher yields is also ongoing (Akçin et al., 2019). Some studies showed that hazelnuts play an important role in converting agricultural by-products into value-added materials. The use of waste hazelnut shell ash (HSA) as an alternative sustainable stabilizer is currently being also investigated in road and building construction studies (Baran et al., 2020; Yurt et al., 2022; Tanyıldızı et al., 2024) Although hazelnut shells are considered an environmentally friendly fuel as biomass, ash waste must be managed appropriately. In this case, serious environmental problems can be eliminated. When nuts such as hazelnut, walnuts, almonds, apricot pit, cashew nut and pistachios are burned, the organic components are lost, leaving behind inorganic minerals (Özyiğit et al., 2022; Leite et al., 2023; Demir, 2026). In particular, hazelnut shells converted into ash through controlled combustion provide a mineral rich material. Preliminary studies indicated that such bio-based ashes have the potential to function as environmentally friendly corrosion inhibitors by forming protective layers on metals and reducing the rate of electrochemical reactions in aggressive environments such as aqueous solutions containing chloride ions. This approach not only offers a sustainable alternative to traditional synthetic inhibitors, but also contributes to the valorization of agricultural waste in line with green chemistry and circular economy principles. Hazelnut shells contain lignin, cellulose, hemicellulose, and various organic compounds. Raw shells can be used as a corrosion inhibitor in ash form after thermal treatment. HSA, in particular, may be more effective in increasing corrosion resistance because it contains the main inorganic components (K, Ca) that can cause galvanic corrosion. This study has detailed the role and mechanism of action of adsorption occurring at the material/solution interface on the electrochemical corrosion mechanism. However, studies showing that hazelnut shell ash can prevent the corrosion of heavy metals are limited. In this study, in order to shed light on the basic corrosion mechanism, it is aimed to clarify this issue by examining the corrosion behavior of iron in a neutral environment using electrochemical techniques (OCP, EIS, Tafel) and solution (ICP-MS) analysis. Considering the increase in hazelnut production, this study was conducted with a view to transforming hazelnuts into value-added products and eliminating any waste that may be generated. However, studies on the corrosion inhibiting effects of hazelnut shell ash on metals are quite limited in the literature. In this study, the effect of hazelnut shell ash on the corrosion behavior of iron metal was investigated with the aim of evaluating hazelnut shells, which are produced as a result of increasing hazelnut production, from an environmental perspective. Electrochemical methods such as open-circuit potential (OCP), electrochemical impedance spectroscopy (EIS), and Tafel polarization techniques were used to elucidate the corrosion mechanism of iron in a neutral environment. Furthermore, the concentrations of metal ions in the solution environment were determined by ICP-MS analysis and evaluated with supporting data on the corrosion process. Additionally, it shows that hazelnut shell ash can inhibit iron corrosion at certain rates and that this agricultural waste can be evaluated as a high added-value, environmentally friendly corrosion inhibitor.

MATERIAL AND METHOD

The electrochemical experiments were performed using a triple electrode system. In this system, iron (Fe, nail) was used as the working electrode, silver-silver chloride

(AgAgCl) electrode as the reference electrode, and platinum (Pt) electrode as the counter electrode. This system was set up using a CHI 660 B potentiostat device (CHI 660 B Model, Inc., Austin, USA) with a temperature-controlled thermostat (WB-110 Model, VAC/220, 50/60 Hz, Wertheim-Germany) and double-walled glass vessels containing 80 mL solution cells, and the experiments were performed using the triple electrode system. All experiments were repeated at least three times and performed using electrochemical methods at 25°C.

Preparation of The Electrodes: The reference electrode (Ag/AgCl, CI^-(sat.), 4M, BASi) was used as reference electrode given in Figure 1a. The counter electrode prepared in the laboratory (Rod, Pt, 2 mm×4 cm) with tightly passing it through Teflon tube with epoxy resin given in Figure 1b. The working electrode (Rod, Fe, 5 mm×5 cm) was prepared by screwing one end with 2 mm brass material, so that the other end could be immersed in the working solution with an air exposed surface area of 0.19625 cm² given in Figure 1c.

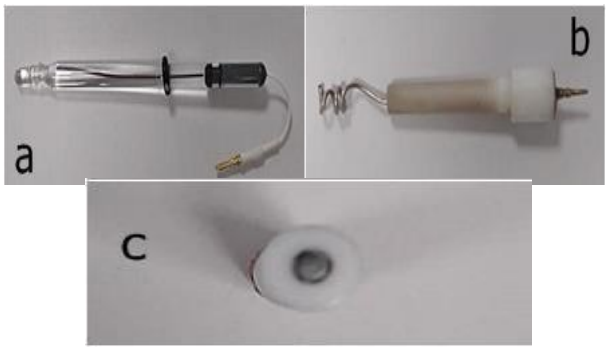

Figure 1. a) Reference electrode (Ag/AgCl) b) Counter electrode (Pt) with Teflon tube c) Working electrode (Fe) in Teflon tube.

Preparation of Study Solutions: The corrosion parameters of the iron electrode in a neutral 1%NaCl environment were investigated using Hazelnut shell ash (HSA). For this purpose, 15 g of HSA was first dissolved in 150 mL of water; the mixture was left to stand at 50°C for one day and then at 25°C for another day. After the standing process, the solution was filtered using a funnel and filter paper under laboratory conditions. The solid residues remaining on the filter paper were not used in the experiments and were stored in appropriate waste containers. The HSA solutions of different concentrations were prepared using the filtrate obtained. In this context, 3.34% v/v, 8.34% v/v, and 25% v/v HSA were taken from the filtrate, respectively, and each was completed to total volume of 300 mL with 1% NaCl solution. The pH determined for all concentrations under laboratory conditions before and after all electrochemical measurements.

Preparation of HSA Samples: Hazelnut shells were collected from the Fındıklı district of Rize in Türkiye. The raw shells were initially crushed using a roller crusher until the particle size was reduced to below 4 mm. The crushed material was then thoroughly washed with deionized water to remove fine particulates and surface impurities. After washing, the shells were oven-dried to remove residual moisture. The dried biomass was subsequently calcined at 450°C for 7 h to produce HSA (Aydemir et al., 2022). The resulting ash was allowed to cool to room temperature inside the furnace to prevent thermal shock. The cooled ash was then ground using Sinbo-brand laboratory grinder until a powder with a particle size comparable to cement fines was obtained. Finally, the ash was stored in airtight containers in the dark at the Corrosion Laboratory to prevent moisture uptake prior to use in corrosion experiments. Electrochemical experiments were carried out under standard laboratory conditions. The prepared HSA was used to investigate its corrosion inhibition performance on iron in the selected test solutions. The appearance of the hazelnut shell ash obtained from the Fındıklı district of Rize is presented in Figure 2.

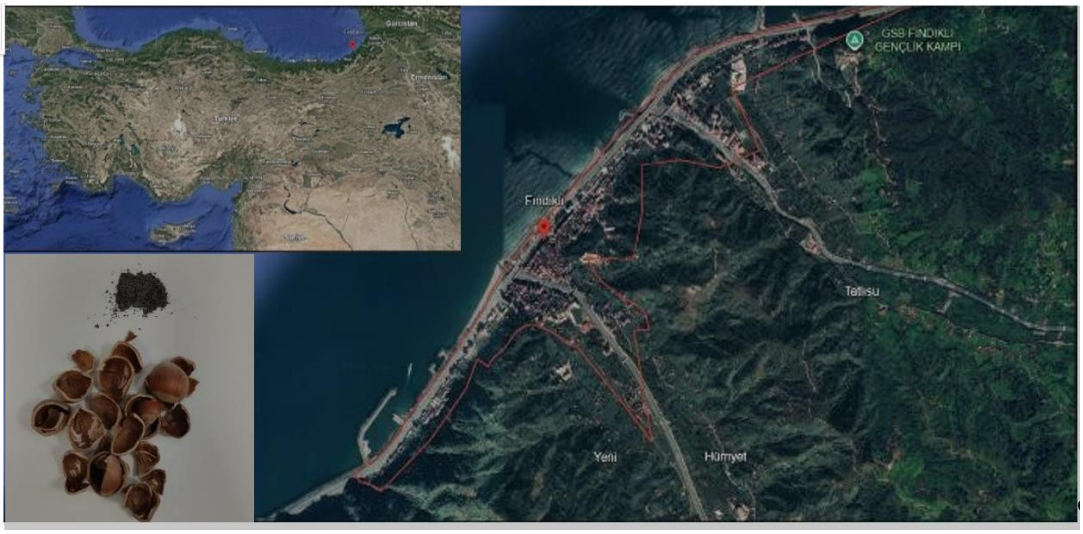

Figure 2. Powdered Hazelnut Shell Ash (HSA) all samples obtained from the Fındıklı district of Rize province from the gardens collected between 2023 and 2024.

Filtration Process of HSA Samples: For the filtration process, under laboratory conditions, hazelnut shell ash was first ground into powder. The ash was then mixed in a 1% NaCl solution and left to stand for one day (24 hours) at 50°C. To maintain the working temperature, this mixture was left for a second day (48 hours). The resulting mixture was filtered. For the working solutions, 3.34% (v/v), 8.34% (v/v) and 25% (v/v) (25 % HSA) were taken from the filtrate and made up to 300 mL with distilled water. The solid residue remaining on the filter paper was not used in this study. Representation samples of the HSA shown in Figure 3.

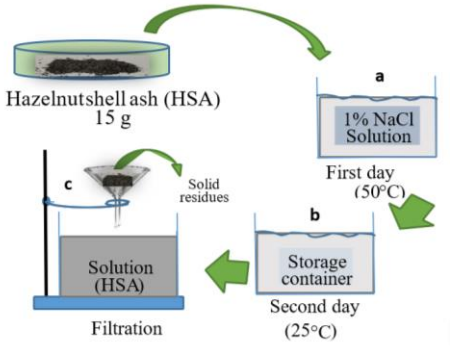

Figure 3. Schematic filtration process of HSA suspension: a) Homogenization of the sample solution for 24 h/50°C, b) for 48 h/25°C, c) Separation of the filtrate and solid phase.

RESULTS AND DISCUSSION

Potential-Time Curves (OCP): The change in potential with time (E_{ocp}-vs.Time) was monitored for all HSA concentrations over a specific period, and it was observed that the potential reached a steady state after approximately 20 minutes. A negative shift in potential was detected at all concentrations. This shift was most likely caused by the interaction of aggressive chloride (Cl^-) ions present in the environment with the metal surface, which made the surface more susceptible to corrosion. However, at a higher concentration (25 % HSA), the potential stabilized around −0.50 V in a shorter time (approximately 200 seconds) compared to other environments. This behavior can be explained by the rapid adsorption of HSA molecules onto the metal surface at higher ash concentrations, which results in an inhibitory or protective effect. In contrast, at lower concentrations (3.34% HSA), chloride ions exhibit a more dominant and aggressive behavior, causing the metal surface to become more vulnerable to corrosion. E_{ocp} curves for all concentrations is shown in Figure 4.

In general, it was determined that the potential varied between −0.45 V and −0.62 V in all concentrations and that a shift of approximately 170 mV in the cathodic direction occurred. However, at the lowest concentration (3.34% HSA), the potential showed a more abrupt and pronounced drop from −0.45 V to −0.60 V compared to other environments. This OCP curves showed that potential rapid decline (8.34% HSA) indicated in red. This was caused by the rapid accumulation of species on the surface.EIS and Tafel polarization curves were obtained to better understand the effect of HSA solutions on the surface and to evaluate the electrochemical behavior in detail.

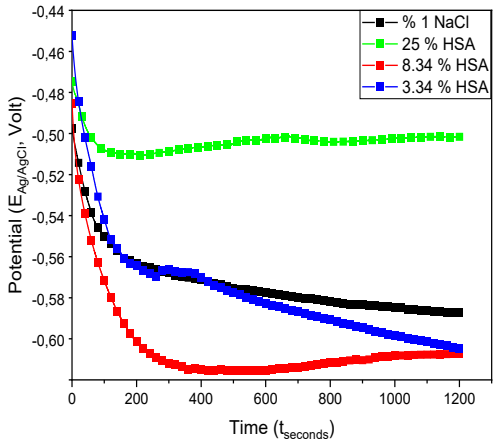

Figure 4. OCP curves for Fe metal immersed in 1% NaCl solution for 1200 seconds with 25 %, 8.34 % and 3.34 % HSA solutions.

Electrochemical Impedance Spectroscopy (EIS): Electrochemical Impedance Spectroscopy (EIS) provides information about the course of the reaction occurring on the surface. This method determines the resistance of the reaction occurring athe metal/solution interface. This resistance had a specific value on both the imaginary (Z''imaginer) and real (Z'real) axes at all frequencies per unit surface area throughout the experiment. Both resistances were obtained for HSA solutions in a specific frequency range of 0.01Hz-100kHz. The EIS curves for HSA solutions, which are the impedance curves occurring on the surface, are given in Figure 5.

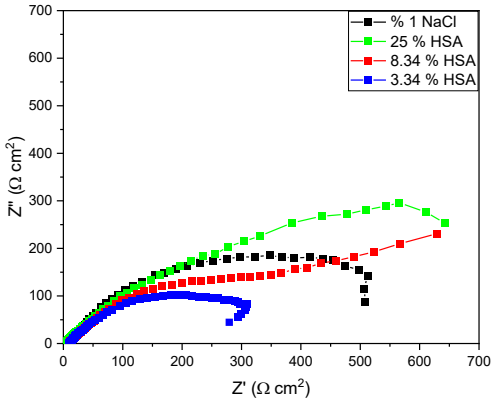

Figure 5. EIS curves for Fe metal immersed in 1% NaCl solution with 25 %, 8.34% and 3.34% HSA solutions.

The virtual resistances corresponding to the peak points of the curves correspond to the maximum frequencies (Yanardağ et al., 2020; Yanardağ, 2024; Yanardağ, 2025). Therefore, a virtual resistance of 100 ohm.cm^2 was obtained at a concentration of 3.34 % HSA, while at 8.34 % it was 125 ohm.cm^2, and at 25 % HSA this resistance reached a value of approximately 300 ohm.cm^2. 8.34% HSA also does not conform to this semicircular pattern. The reason for this is that it showed the separation of the accumulated species from the surface. This also showed that the reaction occurring on the surface was diffusion-controlled. As the concentration increased, the virtual resistance increased. The real resistance was also observed to increase accordingly. However, it was determined that the 3.34 % HSA concentration was closer to completing the semicircle among all the curves. Furthermore, since all the curves tended to complete the semicircle, the EIS curves revealed that the mechanism occurring on the surface was more charge transfer-controlled.

Current-Potential Curves (TAFEL): Current-potential curves were obtained in HSA concentration media. First, currentpotential curves were obtained in 1% NaCl medium without HSA, followed by 25 %, 8.34 % and 3.34 % HSA solution media. The current-potential values were obtained from the CHI 660 B potentiostat device at a scan rate of 0.01 V/s and an amplitude of 5 mV/s. The EIS curves for HSA solutions, which are the EIS impedance curves occurring on Fe, are given in Figure 6.

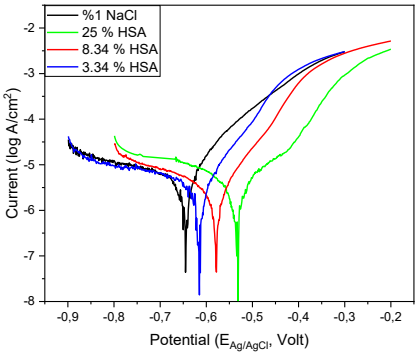

Figure 6. Tafel curves for Fe immersed in 1% NaCl solution with 25 %, 8.34 % and 3.34 % HSA concentrations.

Calculation of Inhibition Activity (φ%): The inhibition effect was obtained using corrosion rates derived from electrochemical methods. Corrosion rates, anodic-cathodic slopes of Tafel curves, and polarisation resistance were obtained directly from the CHI 660 B potentiostat device. The inhibition effect was calculated using the corrosion rates obtained directly and from the currentpotential curves. The inhibition effect was determined from the data obtained from the current-potential curves using the corrosion rate obtained from the Stern-Geary equation. and Inhibition percentages were calculated using the corrosion rates obtained from electrochemical measurements. First, the corrosion rate was determined using the Stern– Geary (S–G) method with Equation-1, using the anodic and cathodic slopes of the Tafel curves obtained from electrochemical measurements and the polarization resistance (Stern et al.,1957).

$$i_{corr}(S-G) = \left[\frac{1}{2.303(1/\beta_a + 1/|\beta_c|)}\right] \cdot \frac{1}{Rp} \qquad \text{Equation-1}$$

Where i_{corr}, β_a, β_c and R_p corresponds to the corrosion rates, anodic slope, cathodic slope and polarizastion resistance of Fe electrode with and without HSA, respectively. Subsequently, the inhibition percentage was calculated using Equation-2 based on the obtained corrosion rates. The equation, both the i_{corr} values obtained from the currentpotential curves (Tafel) and the inhibition data (φ%) using S-G were calculated separately. As a result of this calculation, the percentage effectiveness of the HSA solutions on the Fe electrode was easily calculated (Bolat et al., 2012; Mekonnen, 2026).

$$\mathrm{i_{corr}}(\mathrm{Tafel, S-G}, \varphi\%) = \left[\frac{\mathrm{i_{corr}} - i_{HSA}}{\mathrm{i_{corr}}}\right] \cdot 100 \qquad \text{Equation-2}$$

Where i_{corr} and i_{HSA} corresponds to the corrosion rates of Fe electrode without and with HSA, respectively.

$$R_P(\varphi\%) = \left[\frac{R_p^{HSA} - R_p}{R_p^{HSA}}\right] \cdot 100 \qquad \text{Equation-3}$$

Where R_p and $R_p{}^{HSA}$ corresponds to the corrosion resistance of Fe electrode without and with HSA, respectively. In Equation-3, the φ% values were calculated directly using both the resistance (Rp) obtained from the current-potential (Tafel) method. As a result of these calculations, the values for both methods were calculated and presented in Table 1.

Table 1. Corrosion parameters obtained from the Tafel curves for Fe in 25 %, 8.34 % and 3.34 % solutions prepared with Hazelnut Shell Ash (HSA) in 1% NaCl environment.

Fe	E (Volt)			Slope (mV.dec^{-1})		Rp (Ω.cm^2)	i_{corr} (µA/cm^2)		Inhibition (φ%)		pH	
Solution	E_{ocp}	E_{corr}	ΔE	β_c	β_a	R_p	Tafel	S-G	R_p	Tafel	First	Last
1% NaCl	-0.58	-0.64	-62	527	120	866	0.50	0.49			6.0	5.8
25 % HSA	-0.45	-0.54	-88	186	168	1290	0.26	0.29	33	47	10.2	10.1
8.34 % HSA	-0.57	-0.58	-42	102	403	966	0.39	0.37	10	20	10.5	10.6
3.34 % HSA	-0.59	-0.62	-26	304	722	2450	0.15	0.38	65	70	9.6	9.7

* Hazelnut Shell Ash

ICP-MS Analysis of Metal Ions: Inductively coupled plasma mass spectrometry (ICP-MS, Agilent 7700X) analysis was performed to determine the amount of iron ions in the working solutions. The corrosion behavior of Fe in 1% NaCl solution containing 25 % HSA, 8.34 % and 3.34 % HSA concentrations of hazelnut shell ash (HSA) was evaluated using the ICP-MS analysis for Fe ions detection after the electrochemical experiments. In addition to iron ions, trace amounts of nickel (Ni), chromium (Cr) and cobalt (Co) ions were also found in the HSA solutions. In addition to iron ions, trace amounts of nickel (Ni), chromium (Cr) and cobalt (Co) ions were also found in the HSA solutions. The Cr and Co ion scans in the working solution yielded almost identical results. The metal ion quantities were nearly the same. However, Ni ions were observed more frequently in the environment. This indicates that Ni ions have a lower ability to oxidise in the HSA environment. Fe ions, on the other hand, showed a greater decrease in the presence of HSA compared to Ni, Cr, and Co ions. The retention of metal ions on the surface was largely due to Fe ions. The ICP-MS results were obtained as single concentration values from the analytical measurement, therefore standard deviation values could not be calculated. The ion scan of metal ions in 25 %, 8.34 % and 3.34 % HSA solutions was analysed by ICP-MS and is given in Table 2.

Table 2. ICP-MS analysis of the mass (ppb) of metal ions in in 25 %, 8.34 % and 3.34 % HSA solutions obtained after electrochemical experiments.

Solution HSA*	Fe (ppb)	Ni (ppb)	Cr (ppb)	Co (ppb)
1% NaCl	203	< 112	< 80	< 78
25 % HSA	< 35	< 143	< 80	< 79
8.34 % HSA	< 32	< 153	< 79	< 79
3.34 % HSA	< 22	< 131	< 80	< 79

* Hazelnut Shell Ash.

The number of ions penetrating the surface decreased from 203 ppb to 22 ppb. This indicated the formation of a protective layer on the surface. Furthermore, this situation also proved that HSA acted as an inhibitor. Electrochemical measurements revealed that the lowest HSA concentration (3.34 % HSA) exhibited higher inhibition than the other concentrations. Inhibitions calculated from Tafel polarization and the Stern–Geary (S–G) equation were averaged and ranked as follows: 3.34 % HSA (68%) > 25 % HSA (40%) > 8.34 % (15%) (Table 1). Also, values indicated with "<" represent concentrations below the limit of detection (LOD) of the analytical method. This trend indicated that the 3.34 % HSA solution promotes more effective adsorption on the iron surface, leading to the formation of more coherent and protective film layer. In contrast, higher concentrations did not enhance film stability and instead led to partial disruption of the protective layer. The superior performance of the 3.34 % HSA solution is attributed to the presence of naturally occurring metal oxides in HSA, including K_2O, CaO, MgO, Na_2O, and SiO_2. These oxides act as film-forming constituents and contribute to the development of surface barrier that restricts both anodic dissolution and cathodic reaction kinetics. The formation of this barrier was consistent with previously reported mechanisms for metal-oxide-based inhibitors, where the surface coverage plays a critical role in determining inhibition effect. Solution analysis further supports these findings. Data obtained on the polarization resistance (Rp) of metal ions passing through HSA media (25 %, 8.34 %, 3.34 %) are presented for comparison purposes in Figure 7.

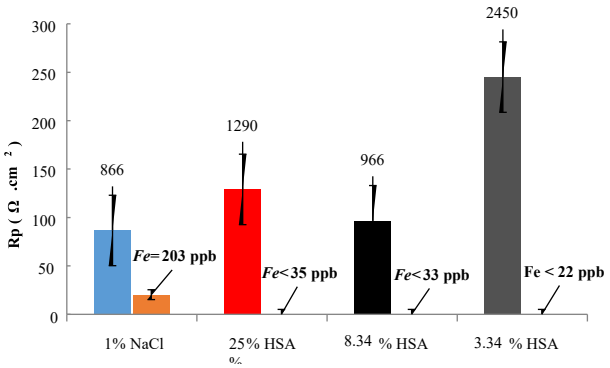

Figure 7. Fe ion concentration detected by ICP-MS analysis and its variation with corrosion resistance.

The increase in the polarisation resistance (R_p) obtained from the Tafel method due to the dissolution of metal ions from the iron surface was obtained in 25 % HSA (1290 Ω cm²), 8.34 % HSA (966 Ω cm²) and 3.34 % HSA (2450 Ω cm²) environments. The increase in resistance occurring on the surface in the working solutions was possible due to the passage of lower iron ions into the environment.

The change in potential over time was monitored in all environments. It was determined that the potential of HSA solutions in 1% NaCl environment, using Fe metal at different ratios such as 3.34 %, 8.34 % and 25 % HSA for 1200 seconds, reached equilibrium as a result of the change in potential over time (Figure 4). From the moment the Fe metal was immersed in the aqueous medium, the open-circuit potential (E_{corr}) shifted approximately 160 mV in the negative direction, from -0.45 V to -0.62 V. This shift occurred more rapidly when 3.34 % of HSA solution was used, and it continued until the end of the waiting period. Therefore, using a smaller amount of HSA solution made surface opening even easier. In the higher concentration HSA solution, the potential change was smaller compared to the initial potential (-0.45 V to -0.50 V). Here, while the 25 % HSA solution stabilized at a more positive potential, the other environments stabilized at more negative potentials. The lowest percentage inhibition from the current-potential (Tafel) method was obtained with 8.34 %

of HSA solution. Polarization resistance increased from 866 Ω cm^2 to 2450 Ω cm^2 in the experiment conducted with 3.34 % of HSA solution, resulting in 65% inhibition. Furthermore, using this method, the potential shifted 20 mV in the anodic direction from -0.640 V to -0.620 V, achieving maximum inhibition of 68%. According to the experimental results, the Tafel and S-G methods confirm each other. As a result of electrochemical experiments, when iron metal was oxidized, the pH of the solution shifted toward the basic side at all HSA concentrations. Therefore, the related electrochemical reaction at the solution/metal interface exposed to the atmospheric environment can be written as follows:

$$Anode: Fe_{(s)} \rightarrow Fe^{2+}_{(aq)} + 2e$$
$$Cathode: O_{2\,(g)} + 2H_2O + 4e \rightarrow OH^-_{(aq)}$$

Consequently, the corrosion of iron metal can be prevented using HSA concentrations. The concentration of dissolved Fe ions in HSA containing media decreased markedly compared to the control. Fe concentrations dropped from 203 ppb to below 35 ppb in the presence of HSA, confirming that the inhibitor effectively suppresses metal dissolution. The reduction in Fe release directly correlates with the formation of stable and adherent surface layer. Although the 25 % HSA solution also showed considerable degree of protection, the higher inhibitor concentration led to the presence of more dissolved corrosion products in the solution. This suggests that at elevated concentrations, the protective film may become less compact or partially porous, allowing for increased interaction between the metal surface and the corrosive environment. Consequently, theintegrity of the oxide-based film appears to be more susceptible to breakdown at higher inhibitor loadings. The results demonstrated that low-concentration HSA solutions provided more stable conditions for effective corrosion inhibition of iron in neutral media. The findings highlight the potential of naturally derived oxide-rich ashes as environmentally benign corrosion inhibitors and emphasize the critical role of concentration in modulating inhibitor performance.

RESULTS

The results clearly demonstrated that corrosion rate of Fe reduced in HSA solutions. The HSA formed a protective layer on the surface, resulting in inhibition. This was because fewer ions were able to pass from the surface into the environment. This decrease occurred as a result of the acidity level of the aqueous environment decreasing, or in other words, an increase in pH. The number of ions penetrating the surface decreased from 203 ppb to up to 22 ppb. The E_{OCP} potential stabilized within a short period (20 minutes) in a 1% NaCl solution at concentrations of 25 %, 8.34 % and 3.34 % HSA. From the moment the Fe metal was immersed in the aqueous medium, the open-circuit potential (E_{corr}) shifted approximately 170 mV in the negative direction, from -0.45 V to -0.60 V. This shift occurred more rapidly when 3.34 % of HSA solution was used, and it continued until the end of the waiting period. Therefore, using a smaller amount of HSA solution made surface opening even easier. In the higher concentration HSA solution, the potential change was smaller compared to the initial potential (-0.45 V to -0.50 V). Here, while the 25 % HSA solution stabilized at a more positive potential, the other environments stabilized at more negative potentials.

Conflicts of interest: The author declares that no conflict of interest.

Ethical approval: This study was conducted within the scope of a research that did not require ethical approval.

REFERENCES

Açkurt, F., Özdemir, M., Biringen, G., & Löker, M. (1999). Effects of geographical origin and variety on vitamin and mineral composition of hazelnut (*Corylus avellana* L.) varieties cultivated in Turkey. *Food Chemistry,* ***65***(3), 309-313. https://doi.org/10.1016/S0308-8146(98)00201-5

Akçin, Y., & Bostan, Z.S. (2019). Effect of Different Irrigation Aplications on Water Activity of 'Tombul' Hazelnut During Storage. *International Journal of Agriculture and Wildlife Science,* ***5***(2), 308-313. https://doi.org/10.24180/ijaws.597163

Alasalvar, C., Amaral, J.S., Satır, S., & Shahidi, F. (2009). Lipid characteristics and essential minerals of native Turkish hazelnut varieties (*Corylus avellana* L.). *Food Chemistry,* ***113***(4), 919-925. https://doi.org/10.1016/j.foodchem.2008.08.019

Aydemir, B., & Yılgın, M. (2022). Investigation of Torrefaction and Combustion Behavior of Hazelnut Shell. *Karadeniz Fen Bilimleri Dergisi,* ***12***(1), 51-65. https://doi.org/10.31466/kfbd.974829

Baran, B., Gökçe, H.S., & Durmaz, M. (2020). Physical and mechanical properties of cement containing regional hazelnut shell ash wastes. *Journal of Cleaner Production*, ***259***, 120965. https://doi.org/10.1016/j.jclepro.2020.120965

Bolat, E., Yanardağ, T., & Küyükoğlu, M. (2012). Corrosion of magnesium modified with different compounds in chloride solution. *Prot Met Phys Chem Surf.* ***48***, 259-264. https://doi.org/10.1134/S2070205112020049

Cartagena, G.N., Araya, M.G., Yanez, S.J. Sepúlveda, G.S., & Pina, J.C. (2023). Influence on physical and mechanical properties of concrete using crushed hazelnut shell. *Applied Sciences*, ***13***(22): 12159. https://doi.org/10.3390/app132212159

Chyhyrynets, O., Sanginova, O., Hu, J., Wu, Y., & He, X. (2025). Optimization of the composition of aluminum phosphate and walnut shell-based composition to increase the corrosion resistance of paint coatings. *Technology Audit and Production Reserves*, ***4***(3(84)), 12-17. https://doi.org/10.15587/2706-5448.2025.334800

Çukur, T., & Çukur, F. (2023). Türkiye'de Fındık Üretimi ve Fındık Fiyatı Arasındaki İlişkinin İncelenmesi. *ÇOMÜ Ziraat Fakültesi Dergisi,* ***11***(2), 253-259. https://doi.org/10.33202/comuagri.1371057

Dai, B., & Ding, Z. (2023). Corrosivity of wood vinegar in bio-oil from hazelnut shells. *Chemistry & Technology of Fuels & Oils,* ***59***(3): 551-560. https://doi.org/10.1007/s10553-023-01555-z

Demir, A. (2026). Evaluation of pistachio (*Pistacia vera* L.) shells: Chemical composition and bioactive potential. *Journal of Anatolian Environmental and Animal Sciences*, **11**, 1-8. https://doi.org/10.35229/jaes.1886041

FAO. (2025). https://www.fao.org/home/search/en/?q=hazelnut

Furtado, L.B., Nascimento, R.C., Henrique, F.J.F.S., Rocha, J.C., Ponciano, J.A.C., & Guimarães, J. M.O.C. (2024). Cashew nut shell liquid (CNSL) residue as a greener corrosion inhibitor: Experimental and DFT studies of intensifier effect. *Journal of Molecular Liquids*, ***406***, 125132. https://doi.org/10.1016/j.molliq.2024.125132

Leite, S.K., & de Carvalho, A.A., Jr., Teixeira, P.R.S., & de Matos, J.M.E. (2023). Cashew Nut Shell Liquid as an Anticorrosive Agent in Ceramic Materials. *Sustainability*, ***15***(11), 8743. https://doi.org/10.3390/su15118743

Mekonnen, K.D. (2026). Corrosion fundamentals: Thermodynamics, rate, passivity, types, and control mechanism. *Results in Surfaces and Interfaces,* ***22***, 100720. https://doi.org/10.1016/j.rsurfi.2026.100720

Ozyigit, I.I., Karahan, F., Yalcin, I.E., Hocaoglu-Ozyigit, A., & Ilcim, A., (2022). Heavy metals and trace elements detected in the leaves of medicinal plants collected in the southeast part of Turkey. *Arab. J. Geosci.* ***15***(1), 1-21. https://doi.org/10.1007/s12517-021-09264-9

Shahmoradi, A.R., Ranjbarghanei, M., Javidparvar, A.A., Guo, L., Berdimurodov, E., & Ramezanzadeh, B. (2021). Theoretical and surface/electrochemical investigations of walnut fruit green husk extract as effective inhibitor for mild-steel corrosion in 1M HCl electrolyte. *Journal of Molecular Liquids,* ***338***, 116550. https://doi.org/10.1016/j.molliq.2021.116550

Stern, M., & Geary, A.L. (1957). Electrochemical Polarization: I. A Theoretical Analysis of the Shape of Polarization Curves. *Journal of The Electrochemical Society*, ***104***(1), 56-63. https://iopscience.iop.org/article/10.1149/1.2428496

Surek, E., & Buyukkileci, A.O. (2017). Production of xylooligosaccharides by autohydrolysis of hazelnut (Corylus avellana L.) Shell. *Carbohydrate Polymers,* ***174***, 565-571. https://doi.org/10.1016/j.carbpol.2017.06.109

Şeker, M.E. (2023). Elemental analysis and health risk assessment of different hazelnut varieties (Corylus avellana L.) collected from Giresun-Turkey, *Journal of Food Composition and Analysis,* **122**, 105475. https://doi.org/10.1016/j.jfca.2023.105475

Tanyıldızı, M., Nasıroğlu, S., Zeybek, A., & Gökalp, İ. (2024). Sustainable use of waste hazelnut shell ash in road construction to stabilize expansive subgrade, *Construction and Building Materials,* **432**, 136663. https://doi.org/10.1016/j.conbuildmat.2024.136663

Topuz, M., Coşkun Topuz, F., Dikici, B., & Seifzadeh, D. (2025). Sustainable walnut shell-filled polylactic acid–hydroxyapatite hybrid coatings for enhanced corrosion resistance and bioactivity of magnesium biomaterials. *Journal of Applied Polymer Science. Advance Online Publication*. ***142***(33), e57321. https://doi.org/10.1002/app.57321

TÜİK. (2024). Bitkisel üretim istatistikleri, https://data.tuik.gov.tr/Bulten/Index?p=Bitkisel-Uretim-1.Tahmini-2025-53940, Erişim tarihi: 09.12.2025.

Yurt, Ü., & Bekar, F. (2022). Comparative study of hazelnut-shell biomass ash and metakaolin to improve the performance of alkali-activated concrete: A sustainable greener alternative, *Construction and Building Materials,* ***320***, 126230. https://doi.org/10.1016/j.conbuildmat.2021.126230

Yanardağ, T. (2024). Synergistic Effect of Plant-Derived Compounds on Corrosion of cp-Ti in Artificial Oral Media: An Experimental and Theoretical DFT Approach. *Prot Met. Phys. Chem. Surf.,* ***60***, 764-776. https://doi.org/10.1134/S2070205124702058

Yanardağ, T. (2025). The Effect of α-Pinene and Fluoride against Corrosion on cp-Ti in Artificial Oral Solution: Experimental and DFT Study. *Prot Met Phys Chem Surf.,* ***61***, 224-236. https://doi.org/10.1134/S2070205125700133

Yanardağ, T., Bayraktar, N., Kahraman Yanardağ, Y., Özgen, Y., & Aksüt, A.A. (2020). The inhibitor effects of *Cannabis sativa* L. extracts on the corrosion of aluminium in H_2SO_4 solutions. *Communications Faculty of Sciences University of Ankara Series B: Chemistry and Chemical Engineering,* ***62***(1), 12-22. https://dergipark.org.tr/en/pub/communb/issue/52583/749033